Heliyon 10 (2024) e30603

Contents lists available at ScienceDirect

Heliyon

journal homepage: www.cell.com/heliyon

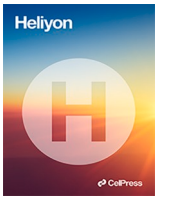

Research article

Tumor suppressor function of RBMS3 overexpression in EOC associated with immune cell infiltration

Tian Yin [a,b,1], Ying Zhang [a,1], Yue Zhao [a,b], Xinyi Zhang [a], Shuqi Han [a], Yixiao Wang [a], Bo Yang [a,*]

[a] *Departments of Oncology Gynecology, The First Affiliated Hospital of Bengbu Medical University, No. 287 Changhuai Road, Bengbu, 233004, China*

[b] *Anhui Engineering Technology Research Center of Biochemical Pharmaceutical, Bengbu Medical University, Bengbu, Anhui Province, China*

ARTICLE INFO

Keywords:
Epithelial ovarian cancer
RBMS3
Tumor microenvironment
Immune infiltration
Immunotherapy

ABSTRACT

Objectives: Epithelial ovarian cancer (EOC) is considered to be a prevalent female malignancy with both high incidence and mortality. It is reported that RNA-binding protein 3 (RBMS3) executives a tumor suppressor function in different cancers. This investigation was designed to examine the expression of RBMS3 in epithelial ovarian cancer, the effects on EOC cells, and its connection to immune cells that infiltrate tumors in the EOC microenvironment.

Methods: The expression levels of RBMS3 in EOC tissues as well as their correlations with immune cell infiltration and clinical outcome were examined using bioinformatics approaches. Western blotting as well as immunohistochemistry were carried out to determine the protein levels in EOC tissues. In addition, qRT-PCR was employed to look at the expression of the mRNA. The role of RBMS3 in EOC cells was investigated, and an RBMS3 lentiviral vector was developed. The effects of RBMS3 on subcutaneous tumor development, the proliferation protein Ki-67, the tumor angiogenesis indicator CD31, and its function in controlling the tumor immune microenvironment were evaluated by *in vivo* tests.

Results: There was a considerable decrease in RBMS3 expression in EOC tissues, which was linked to a poor prognosis for patients and the infiltration of multiple immune cell. Given immunohistochemical studies, tissues with increased RBMS3 expression had decreased markers of myeloid-derived suppressor cells, regulatory T cells, and M2 macrophages, whereas M1 macrophage markers were elevated. RBMS3 appears to suppress the capabilities of proliferating, invading, and migrating in EOC cells according to *in vitro* tests, whereas tumors overexpressing RBMS3 developed more slowly in syngeneic mouse models. The overexpression of RBMS3 led to a decline in the levels of Ki-67 protein and CD31. Additionally, it showed a negatively correlation with markers of regulatory T cell, myeloid-derived suppressor cell, and M2 macrophage but a positive correlation with markers of M1 macrophage.

Conclusions: The findings revealed that elevated RBMS3 expression plays a tumor suppressor role in EOC and was connected to patient survival in EOC. The studies conducted *in vitro* and *in vivo* demonstrated a link between RBMS3 expression and the infiltration of certain immune cells, indicating a function for RBMS3 in the immunosuppressive tumor microenvironment and its promising efficiency as a novel target for immunotherapy against EOC.

* Corresponding author.
E-mail address: yangbo@bbmc.edu.cn (B. Yang).

[1] These authors have contributed equally to this work and share first authorship.

https://doi.org/10.1016/j.heliyon.2024.e30603
Received 15 February 2024; Received in revised form 28 April 2024; Accepted 30 April 2024
Available online 1 May 2024

1. Introduction

Data from the International Agency for Research on Cancer (IARC) GLOBOCAN reveals that there were 313,959 cases reported of ovarian cancer and 207,252 fatalities from the disease in 2020 [1]. Ovarian cancer has the poorest prognosis and highest death rate among all gynecological malignancies, despite ranking tenth in the world for both morbidity and mortality among cancers that affect women [2]. Considering there are no distinct symptoms in the initial phases of the illness and there are no reliable screening methods, the majority of patients receive their diagnosis when the tumor has already widely metastasized [3,4]. The majority of patients have recurrence after a few years of treatment and ultimately succumb to chemotherapy-resistant illness, despite the success of cytoreductive surgery and chemotherapy (carboplatin and paclitaxel) [5,6]. Less than 50% of women survive for more than five years as a result of these difficulties, which leads to an extremely low overall survival rate (OS) [7]. This seriously impedes the effort to cure this cancerous growth.

Studies have revealed that the tumor immune microenvironment (TIME) is crucial for cancer growth as well as therapy. The TIME of ovarian tumors consists of multiple cell types, comprising of tumor, immune, and mesenchymal stromal cells, in addition to cytokines and the metabolites that are linked with them, just like other tumor types. Ovarian cancer formation, progression, and metastasis are linked to disruption of the TIME [8,9], and immunosuppressive microenvironments have been shown to lower the effectiveness of immunotherapy [10], which has a negative impact on patient outcomes. This implies that increasing the effectiveness of EOC therapy may require overcoming the TIME [11]. Thus, to find novel biomarkers and therapeutic targets, a thorough analysis of the underlying factors and immunologic factors linked to EOC development is urgently needed.

RNA-binding protein 3 (RBMS3), additionally known as RNA-binding motif, single-stranded interacting protein 3, first came to light by Penkov et al. The gene was identified to be positioned in the p23–p24 region of human chromosome 3 and to be a tumor suppressor gene (TSG) [12]. It is a component of the c-Myc single-chain binding protein (MSSP) family and is involved in DNA replication, gene transcription, apoptosis, and the advancement of the cell cycle [13]. According to recent studies, RBMS3 has a major function in the occurrence and progression of a few of illnesses, including liver fibrosis, in addition to regulating cell biological process. In addition to controlling bone cell proliferation and differentiation, RBMS3 is crucial for the formation of the mouse pancreas [14–16]. Additionally, It has been proposed that RBMS3 indicates a major involvement in tumor pathogenesis. For instance, minimized expression of RBMS3 has been attributed to a dismal prognosis for esophagus and lung squamous cell carcinomas, as well as cancers of the breast, gallbladder, and stomach [17–21]. Further research has revealed that RBMS3 can delay the degeneration of intervertebral discs by blocking the Wnt/β-catenin signalling pathway) [22] and regulating the epithelial-mesenchymal transition (EMT) [23]. Findings concluded by Lv et al. [24] reveal that activation of the LKB1/AMPK pathway raised RBMS3 expression, which in turn stopped lung cancer from spreading. The precise regulation mechanism of RBMS3 in tumor is unclear, and the relevance of this protein in EOC has not been well-studied. According to Wu et al. [25], ovarian cancer became more resistant to cisplatin when RBMS3 was deficient because it activated the Wnt/β-catenin/CBP signalling pathway. In addition, Wang et al. [26] proposed that RBMS3 functions as a tumor suppressor gene and could be a promising biological indicator for prognostic prediction. Despite the apparent importance of RBMS3 in the initiation of various cancers, its function in epithelial (EOC) and how it relates to tumor immunity remains unclear, and in-depth research is still required.

This study examined the expression level of RBMS3 in EOC and its effect on patient prognosis using Gene Expression Profiling Interactive Analysis (GEPIA) as well as the Kaplan-Meier (KM) plotter. The TISIDB (an integrated repository portal for tumor-immune system interactions) database and immunohistochemistry (IHC) were employed to investigate the relationships that exist between OC's tumor immune microenvironment (TIME) and RBMS3. Furthermore, the biological roles of RBMS3 in EOC and its connections with tumor-infiltrating immune cells were investigated. The results establish the foundation for a thorough comprehension of RBMS3's role in EOC and its connection to the TIME. According to this research, RBMS3 may be a viable therapeutic target, providing OC patients with an innovative approach to treatment.

2. Materials and methods

2.1. Patient recruitment and sample collection

Between January 2018 and November 2020, the First Affiliated Hospital of Bengbu Medical University provided sixty samples of EOC tissue and thirty samples of normal ovarian tissue. All specimens were taken during surgery. Surgical pathology confirmed the tumor specimens, which were from individuals with primary EOC diagnoses. Patients who underwent oophorectomy for benign gynecological disorders had normal ovarian tissues removed. In anticipation of further processing, the samples were promptly frozen in liquid nitrogen and stored under a condition of −80 °C. The First Affiliated Hospital Ethics Committee of Bengbu Medical University accepted the study protocol (Approval No.: 2023YJS126) and all subjects gave informed consents. The following were the inclusion criteria: (1) Pathology-confirmed diagnosis of EOC; (2) No immunotherapy, chemotherapy, or radiation had been administered before to surgery. The following were the exclusion criteria: (1) The existence of further malignant growths; (2) The existence of illnesses impacting vital organs.

2.2. Immunohistochemistry (IHC)

Tissue samples were embedded in paraffin, cut into 4-μm slices, deparaffinized, and then rinsed with water. For antigen repair,

sodium citrate buffer (1 mM, pH 6.0) was employed. This was followed by three PBS washes lasting 5 min each, a 15-min immersion in a 3% hydrogen peroxide solution, and an additional three PBS washes lasting 5 min each. Following antigen repair and an incubation period of 3% hydrogen peroxide, the tissues were blocked for 30 min under a condition of the room temperature using 10% sheep serum. After that, the sections were incubated for overnight under a condition of 4 °C with a rabbit polyclonal antibody against RBMS3 (No.: ab198248; Abcam, UK). The sections were rinsed with PBS three times, and then they were incubated with the secondary antibody (No.: GB23303; Servicebio, Wuhan, China) for 60 min before being rinsed with PBS. The sections were incubated under a condition of the room temperature with 3,3′-diaminobenzidine (DAB) (No.: G1212; Servicebio, Wuhan, China), counterstained with hematoxylin, and sealed after a 20-min water washing to halt color development. Two pathologists rated the RBMS3 staining intensity and independently analyzed the data. The homogeneity of dyed cells was initially assessed using low-power microscopy, and subsequently determined by randomly selecting five fields at high power (× 200). One might grade the staining intensity in four distinct ways: 0, no staining; 1, light yellow staining; 2, yellow staining; and 3, tan staining. The percentages of positive cells were 1 (10–50%), 2 (50–70%), 3 (more than 75%), and 0 (less than 10%). The staining intensity score was multiplied by the ratio of positive cells to generate the staining index, which ranged from 0 to 9. A result of $\leq$6 indicated low or negative expression, whereas values ranging from 6 to 9 indicated medium-high expression.

2.3. Cell culture and lentiviral transfection

Shanghai Jinyuan Biotechnology Co., Ltd. provided the mouse EOC cell line ID8 (No.: JY049; Jinyuan, Shanghai, China). In an incubator set at 37 °C with 5% CO_2, the cells were cultivated in Dulbecco's Modified Eagle Medium (DMEM) supplemented with 10% fetal bovine serum and 1% penicillin/streptomycin. Heyuan Biotechnology (Shanghai, China) provided the lentiviral vectors Lv-RBMS3, Lv-Vector, and Lv-shRBMS3, together with their control vector Lv-shNC. Lentiva virus was introduced into the ID8 cells at a multiplicity of infection (MOI) of around 20. Lentivron-mediated RBMS3 short hairpin RNA interference (Lv-shRBMS3) was used to knock down RBMS3 in ID8 cells, and lentiviral vector (Lv-Vector) or lentivirus (Lv-RBMS3) was used to induce overexpression. To establish stable expression cell lines, 2.5 μg/mL puromycin was used to pick up the transfected cells. We assessed the expression of RBMS3 with the assistant of Western blotting and qRT-PCR. Table 3 provides the shRNA sequences of the lentiviral construct knockdown cell lines.

2.4. Extraction of total RNA, reverse transcription, and qRT-PCR

TRIzol (No.: TQ102-01; Xinbei, Shanghai, China) was employed to extract the RNA, and spectrophotometry was implemented to detect the RNA's concentration and purity. Using the NovoScript Plus All-in-one 1st Strand cDNA Synthesis SuperMix (gDNA Purge) kit (No.: E047; Novoprotein, Suzhou, China), the RNA was reverse-transcribed to cDNA. On a StepOneTM Real-Time PCR machine (Applied Biosystems; Thermo Fisher, Waltham, MA, USA), the cDNA was amplified using the NovoStart SYBR qPCR SuperMix Plus reagent (No.: E096; Novoprotein, Suzhou, China). Denaturation was carried out for 1 min at 95 °C, followed by 35–45 cycles of 20 s at 95 °C, 20 s at 60 °C, and 30 s at 72 °C in the qRT-PCR software. The internal reference was GAPDH. Utilizing the comparative threshold cycle ($2^{-\Delta\Delta CT}$) approach, the relative gene expression gene was determined. Table 4 displays the primer sequences that were employed.

2.5. Western blotting

A lysis buffer containing 1 mM phenylmethylsulfonate fluoride (PMSF; No.: BL612A; Beijing Labgic Technology Co., Ltd., China) was applied to extract the total protein using RIPA (No.: P0013B; Shanghai Beyotime Biotech Co., Ltd., China). Using a fast preparation kit (No.: ZJ102; Shanghai Yazy Biomedical Technology Co., Ltd., China), after samples were electrophoretically separated on 10% SDS-PAGE gels, they were transferred to PVDF membranes for 80 min at a constant current of 200 mA. Prior to being incubated with primary antibodies against RBMS3 (1:2000; No.: DF8599; Affinity Biologicals, China) or GAPDH (1:10,000; No.: AF7021; Affinity Biologicals, China) for an entire night on a shaking table at 4 °C, for 2 h under a condition of the room temperature, 5% skim milk was applied to block the membranes. After that, they had three TBST washes (10 min each wash). The following step involved incubating an anti-rabbit secondary antibody coupled with horseradish peroxidase for 1 h under a condition of the room temperature. After that, the PVDF membranes were found using the ECL-chemiluminescent kit (No.: BL520A, Biosharp, Beijing, China) and quantified using ImageJ software from IBM Corp. (Armonk, NY, USA).

Table 1
Expression of RBMS3 in EOC and normal tissue.

	Total	RBMS3 Expression	
		Low	High
Tumor tissues	60	39	21
Normal tissues	12	2	10

Table 2
The relation between clinical parameters and the expression of RBMS3.

Clinical parameters		Low	High	*P* value
Age (year)	<58	20 (51.3 %)	12 (57.1 %)	0.664
	≥58	19 (48.7 %)	9 (42.9 %)	
Tumor Size/cm	<9	21 (53.8 %)	9 (42.9 %)	0.417
	≥9	18 (46.2 %)	12 (57.1 %)	
FIGO stage	I-II	8 (20.5 %)	10 (47.6 %)	0.029
	III-IV	31 (79.5 %)	11 (52.4 %)	
CA125(U/mL)	<512	20 (51.3 %)	10 (47.6 %)	0.787
	≥512	19 (48.7 %)	11 (52.4 %)	
Retroperitoneal lymph node metastasis	No	35 (89.7 %)	19 (90.5 %)	0.928
	Yes	4 (10.3 %)	2 (9.5 %)	
Histological grading	High-grade	32 (82.1 %)	12 (57.1 %)	0.037
	Low-grade	7 (17.9 %)	9 (42.9 %)	
Residual lesion size/cm	0	6 (15.4 %)	5 (23.8 %)	0.449
	≤1	20 (51.3 %)	12 (57.1 %)	
	> 1	13 (33.3 %)	4 (19.0 %)	

Table 3
shRNA sequences.

Marker	RNA sequence
Lv-shNC	CCTAAGGTTAAGTCGCCCTCG
Lv-shRBMS3-1	GCAAGACCCTACGAATCTATA
Lv-shRBMS3-2	AGCCCTTTGGACACGTGATAT
Lv-shRBMS3-3	TGAAGTGGTGATTCAACATTT

Table 4
Primer sequences.

Gene	Species	Primer
RBMS3 Forward	Human	ACTGAAAAATGTGAAGTGGTAATTC
RBMS3 Reverse	Human	CTTCTTTTGTCCTCCATCAGCG
GAPDH Forward	Human	GGAGCGAGATCCCTCCAAAAT
GAPDH Reverse	Human	GGCTGTTGTCATACTTCTCATGG
RBMS3 Forward	Mouse	CTGGCATGGCTCTGACCTATGAC
RBMS3 Reverse	Mouse	TGCGGTTGGTTGCGAGACTG
GAPDH Forward	Mouse	AGAAGGTGGTGAAGCAGGCATC
GAPDH Reverse	Mouse	CGAAGGTGGAAGAGTGGGAGTTG

GAPDH, glyceraldehyde-3-phosphate dehydrogenase; RBMS3, RNA Binding Motif Single Stranded Interacting Pritein 3; RT-qPCR, Reverse Transcription Quantitative PCR.

2.6. Cell viability assays

Utilizing the Cell Counting Kit-8 (CCK-8) assays, the effects of RBMS3 on ID8 cell proliferation were assessed. Six duplicate wells per set of cells in the logarithmic growth phase were seeded in 96-well plates at a density of 3×10^3/100 μL/well. Following the 24-48-72 h incubation period, 10 μL of the CCK-8 test solution was applied to each well, and the incubation was performed at 37 °C in the dark for an additional 2 h. We used a Microplate Reader (Synergy HT, BioTek, USA) to evaluate the optical density (OD) values at 450 nm. Three iterations of this experiment were conducted.

2.7. Colony formation assays

Six-well plates were seeded with exponentially growing ID8 cells, which were then cultivated in DMEM supplemented with 10% FBS. Every 72 h, the culture media was replaced once the cells had attached themselves to the plates. Once the colonies became visible after two weeks, they were counted, photographed, and examined under an optical microscope. The colonies were then washed thoroughly with PBS, fixed in 4% paraformaldehyde for 20 min, and stained with crystal violet for 30 min, and then rinsed with PBS. The colony numbers were shown as the three separate experiments' mean ± standard deviation (SD).

2.8. Wound healing assays

The produced cell lines were planted onto 6-well plates with 2.5×10^5 cells per well and cultivated until a monolayer formed. Following a linear scratch in the cell monolayer using a sterile 200 μL micropipette tip, PBS washing was performed to eliminate the

cell debris. An inverted microscope was used to detect cell migration and take pictures of the wound 0, 24, and 48 h after scratching. ImageJ software was implemented to determine the relative migration rate of the cells in each group.

2.9. Transwell assays for cell migration and invasion

For the migration experiment, Transwell tools were employed to re-suspend cells (3×10^4 cells/well) in serum-free medium and implant them into the top chamber of a 24-well plate. The lower chamber had 600 μL of medium containing 15% FBS. After being cultured for 24 h at 37 °C, the cells that had migrated to the lower chamber were washed with PBS, fixed for 20 min with 4% paraformaldehyde, and stained for 30 min with 0.4% crystal violet. For the invasion experiment, in the upper chamber, cells were cultured in serum-free media using 40 μL of Matrigel (No.: HY-K6001; MedChemExpress, NJ, USA). In the lower chamber, 600 μL of culture solution containing 15% FBS was applied to measure invasion. The upper chamber was removed after a 24-h incubation period at 37 °C, and any cells that had not fallen to the bottom were gently removed using a cotton swab. The cells were then prepared as previously mentioned and stained. Five randomly chosen fields' migratory or invading cells were photographed using light microscopy and counted using ImageJ software.

2.10. Cell cycle analysis

To make sure the cells were in an active condition, they were cultivated until they reached the logarithmic growth phase. Following seeding on 6-well culture plates, the cells (5×10^6 cells/well) were cultured for 24 h at 37 °C with 5% CO_2. After that, the cells were taken out and centrifuged for 5 min to pellet them. They were then twice rinsed with pre-chilled PBS and fixed for 1 h at 4–20 °C by adding drops of pre-cooled ethanol. Following a 10-min centrifugation at 1000*g*, after discarding the supernatant, the cells were collected, washed twice in cold PBS, and then resuspended in cold PBS. Next, a Bebo Biotech cell cycle detection kit (No.: BB-4104; Shanghai, China) was employed. In summary, after being subjected to a 20 μL RNase A solution, the cells were incubated for 30 min at 37 °C in a water bath. 400 μL of propidium iodide (PI) were applied to the cells to resuspend them after centrifugation. The cells were gently mixed and then incubated at 4 °C for 30 to 1 h in the dark. The cells were then evaluated using flow cytometry (CytoFLEX, Beckman Coulter, NJ, USA) to determine the proportion of cells in each cell cycle stage. The data is analyzed using the corresponding software based on the flow cytometer results.

2.11. Assessment of cell apoptosis

Transfected ID8 cells were sown in 6-well plates and cultured in a 5% CO_2 and 37 °C incubator for 24 h. The cells underwent trypsinization, centrifugation to gather them, and two cold PBS washes. Following resuspension in 100 μL of 1x Annexin V binding solution, 4 μL of Annexin V-APC staining solution was applied. Next, the cells were gently mixed and incubated for 5–10 min at 2–8 °C in the dark, following the manufacturer's instructions. After that, after applying cautiously mixing 5–10 μL of PI staining solution, the mixture was incubated for 1–3 min at 2–8 °C in the dark. The 1x Annexin V conjugate solution was then applied and carefully stirred. The cells were immediately assessed by flow cytometry after being run through a 300-mesh nylon mesh, and FlowJo 10.0 software was used to analyze the cells for analysis. The experiment was repeated three times.

2.12. Animal model

In this investigation, eight female C57BL/6 mice per group, ages 4–6 weeks, were utilized. Suzhou Xishan Biotechnology Co., Ltd. (License No.: SCXK [Zhejiang] 2019-0002) provided the animals. The mice were kept in a room with food and water, at 25 ± 2 °C and 50 ± 5% humidity. The First Affiliated Hospital of Bengbu Medical University's Animal Research Ethics Committee approved all animal studies (Approval No.: [2023]595), and all animal research complied with institutional, national, and international standards for the humane treatment of laboratory animals. The right neck and back of the mouse were injected with 100 μL of cell suspension/mouse, which contained around 6×10^6 cells, for the subcutaneous tumor model. The cells were placed in a combination of growth factor-reduced basement membrane Matrigel and pre-chilled serum-free DMEM, which was diluted to a final concentration of less than 67% of the total volume of the Matrigel and cell suspension. Every three days, the volume of the tumor and the weight of the mice were recorded. After 28 days, the mice were killed, and the tumor tissues were removed for analysis. The tumors' long and short diameters were measured with vernier calipers, and their weight was recorded using an electronic balance. The volume and morphology of the tumors were captured by photography. One half of the excised tumor tissue was frozen at −80 °C and the other half was preserved in 4% paraformaldehyde. Lastly, investigations using immunofluorescence and immunohistochemistry (IHC) were carried out.

2.13. Immunofluorescence analysis (IF)

The collected tumor tissues were cut into slices using a microtome and then paraffin was fixed. To retrieve the antigen, the sections were dried after being submerged in a EDTA antigen repair buffer (pH 8.0). Blocking serum was applied dropwise to the slices, and they were then incubated for an hour under a condition of the room temperature in a humidified box. The primary antibodies (see below) were subsequently applied to the sections, and they were left overnight at 4 °C. Afterwards, the sections were treated with goat anti-rabbit (H + L) secondary antibodies for 2 h under a condition of the room temperature. Finally, an Olympus BX53 microscope was used to create immunofluorescence images. The primary antibodies used were rabbit anti-INOS (No.: AF0199; Affinity, China), rabbit

anti-ARG1 (No.: DF6657; Affinity, China), rabbit anti-FOXP3 (No.: AF6544; Affinity, China), and rabbit anti-CD11b (No.: DF2911; Affinity, China). Specifications of the main and secondary antibodies used are provided in Table 5.

2.14. Statistical analysis

It was conducted using GraphPad Prism 8.0.2. Image J was applied to analyze the images. The differences between two groups were assessed by *t*-test. For multiple data sets, one-way ANOVA was used. The Spearman's chi-square test (χ^2 test) and the continuity-corrected chi-square test were used to conduct a two-factor correlation study. The survival study was employed using the Kaplan-Meier method. P-values that indicate noteworthy variations and specifics are included in the corresponding figure legends. Three duplicates of each experiment were carried out. $^*P < 0.05$, $^{**}P < 0.01$, $^{***}P < 0.001$ and $^{****}P < 0.0001$.

3. Results

3.1. Expression of RBMS3 is reduced in EOC tissues and is associated with poor prognosis

The first tool that we applied to investigate the RBMS3 expression levels in EOC was GEPIA (http://gepia.cancer-pku.cn/). Following the extraction of pertinent patient data from the database, it was discovered that the EOC tissues had lower amounts of RBMS3 mRNA than the normal tissues (Fig. 1A). Furthermore, the Kaplan-Meier plotter was utilized to examine the clinical significance of RBMS3 in patients with EOC (Lánczky & Győrffy, 2021). The findings showed that, in contrast to patients with low RBMS3 expression, those with high RBMS3 expression had longer progression-free survival (PFS) and overall survival (OS) ($P < 0.05$) (Fig. 1B and C). Subsequently, RBMS3 expression in EOC tissues was investigated by Western blotting (Fig. 1E and F) and RT-qPCR (Fig. 1D). Findings revealed that OC tissues expressed RBMS3 at a considerably smaller amount than normal tissues.

The expression level and location of the RBMS3 protein were then examined using the Human Protein Atlas database (Human Protein Atlas proteinatlas.org). This demonstrated that the cytoplasm is where RBMS3 is found. Next, tissue samples were gathered for immunohistochemistry (IHC) analysis, comprising 60 EOC tissues and 12 normal tissues from patients, to clarify the function and clinical importance of RBMS3. According to the intensity of immunohistochemical staining, Table 1 points out that the cancer tissues were divided into the low-expression group ($n = 39$) and the high-expression group ($n = 21$). Furthermore, it emerged that RBMS3 protein levels were considerably reduced in malignant tissues than in healthy tissues, and it was established that RBMS3 is mostly expressed in the cytoplasm (Fig. 1G). Table 2 shows the relationship between RBMS3 expression and clinical parameters of EOC; there was no significant correlation between RBMS3 expression and patient age, tumor size, CA125 (U/mL), retroperitoneal lymph node metastasis and residual lesion size (all $P > 0.05$), but RBMS3 expression was significantly correlated with FIGO stage ($P = 0.029$) and histological grade ($P = 0.037$). Lastly, Kaplan-Meier survival curves were employed to examine how RBMS3 expression affected patients with EOC's PFS and OS. According to the data (Fig. 1H and I), patients with reduced RBMS3 expression had dramatically shorter OS (hazard ratio, 0.3778; $P = 0.0329$) and PFS (hazard ratio, 0.410; $P = 0.0431$). All things considered, these outcomes revealed that RBMS3 expression is downregulated in EOC tissues and is linked to a bad prognosis for EOC patients.

3.2. RBMS3 surpasses the proliferation, migration, and invasion of EOC cells in vitro

RBMS3's biological activity in EOC cells was further explored by creating ID8 cells with RBMS3 knockdown (Lv-shRBMS3) and overexpression (Lv-RBMS3) using lentivirus-mediated techniques, along with the equivalent control vector cell lines. When green fluorescent protein (GFP) expression was ascertained using fluorescence microscopy 72 h after transduction, the cell state was shown to be normal (Fig. 2A and B). The approach was deemed successful as evidenced by the evaluation of lentiviral transduction efficiency by RT-qPCR (Fig. 2C) and Western blotting (Fig. 2D). Then, colony formation and CCK-8 tests were used to look at cell proliferation. The RBMS3 overexpression group (Lv-RBMS3) exhibited evident decreases in colony formation and vitality, whereas the RBMS3 knockdown group (Lv-shRBMS3-1) demonstrated enhanced cell proliferation. The findings of colony formation and proliferation are displayed in Fig. 2E and F. As indicated by Fig. 2, Scratch and Transwell cell assays were used to detect the role of RBMS3 in migration and invasion. Firstly, it was shown that greater expression of RBMS3 inhibited the migration of ID8 cells in the wound healing

Table 5
Antibody information used in the experiment.

Antibody	Dilution	Supplier	Host species	Catalogue #
RBMS3	IHC 1: 100	Abcam	Rabbit	ab198248;
INOS	IF 1:300	Affinity	Rabbit	AF0199
ARG1	IF 1:300	Affinity	Rabbit	DF6657
CD206	IHC 1:100	Affinity	Rabbit	DF4149
CD11b	IHC 1:200、IF 1:300	Affinity	Rabbit	DF2911
FOXP3	IHC 1:200、IF 1:300	Affinity	Rabbit	AF6544
RBMS3	WB 1:2000	Affinity	Rabbit	DF8599
β-catenin	WB 1:2000	Affinity	Rabbit	AF6266
GAPDH	WB 1:10,000	Affinity	Rabbit	AF7021
Rabbit IgG HRP	WB 1:10,000	Affinity	Goat	S0001

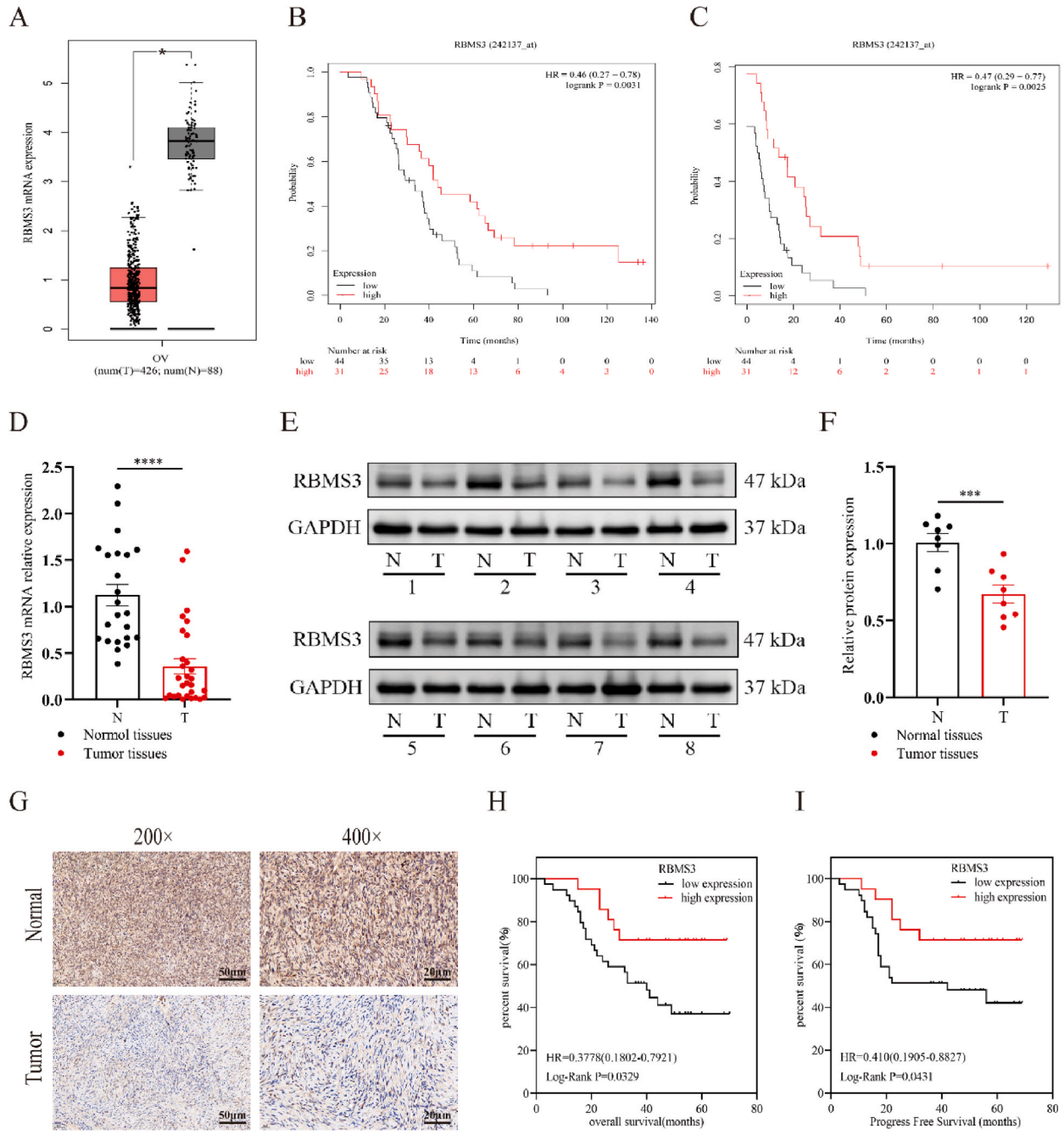

Fig. 1. The poor prognosis of OC patients is linked to down-regulated RBMS3 expression in OC tissues. (A) RBMS3 mRNA expression levels from the GEPIA database in both normal tissue and OC. Grey (n = 88) normal samples and red (n = 426) tumor samples. (B, C)Data on OS and PFS for patients with OC were collected with the assistant of the Kaplan-Meier plotter (https://kmplot.com/analysis/). (D) qRT-PCR was used to measure the mRNA levels of RBMS3 in 29 instances of EOC and 23 cases of normal ovarian tissue. (E, F) Western blot analysis reveals the RBMS3 protein expression level in eight pairs of EOC tissues. (G) Typical IHC staining pictures of RBMS3 in normal tissue (Normal) and OC (Tumor). The scale bars are 50 μm and 20 μm respectively. (H, I) Kaplan-Meier study of the effects of 60 EOC patients' RBMS3 expression on OS and PFS. $^{*}P < 0.05$, $^{**}P < 0.01$, $^{***}P < 0.001$ and $^{****}P < 0.0001$.The uncropped versions of Fig. 1E is in Supplementary Figs. S1 and S2.

experiments, in contrast to the Lv-vector group. On the other hand, cells in the knockdown group (Lv-shRBMS3-1) exhibited greater migratory capacity than those in the Lv-shNC group (Fig. 2G and H). To learn more about how RBMS3 affects ID8 cell migration and invasion *in vitro*, the Transwell technique was employed. ID8 cells' migration and invasion were greatly reduced following RBMS3 overexpression (Fig. 2I and J), but cells in the knockdown group (Lv-shRBMS3-1) displayed enhanced migration and invasion. These

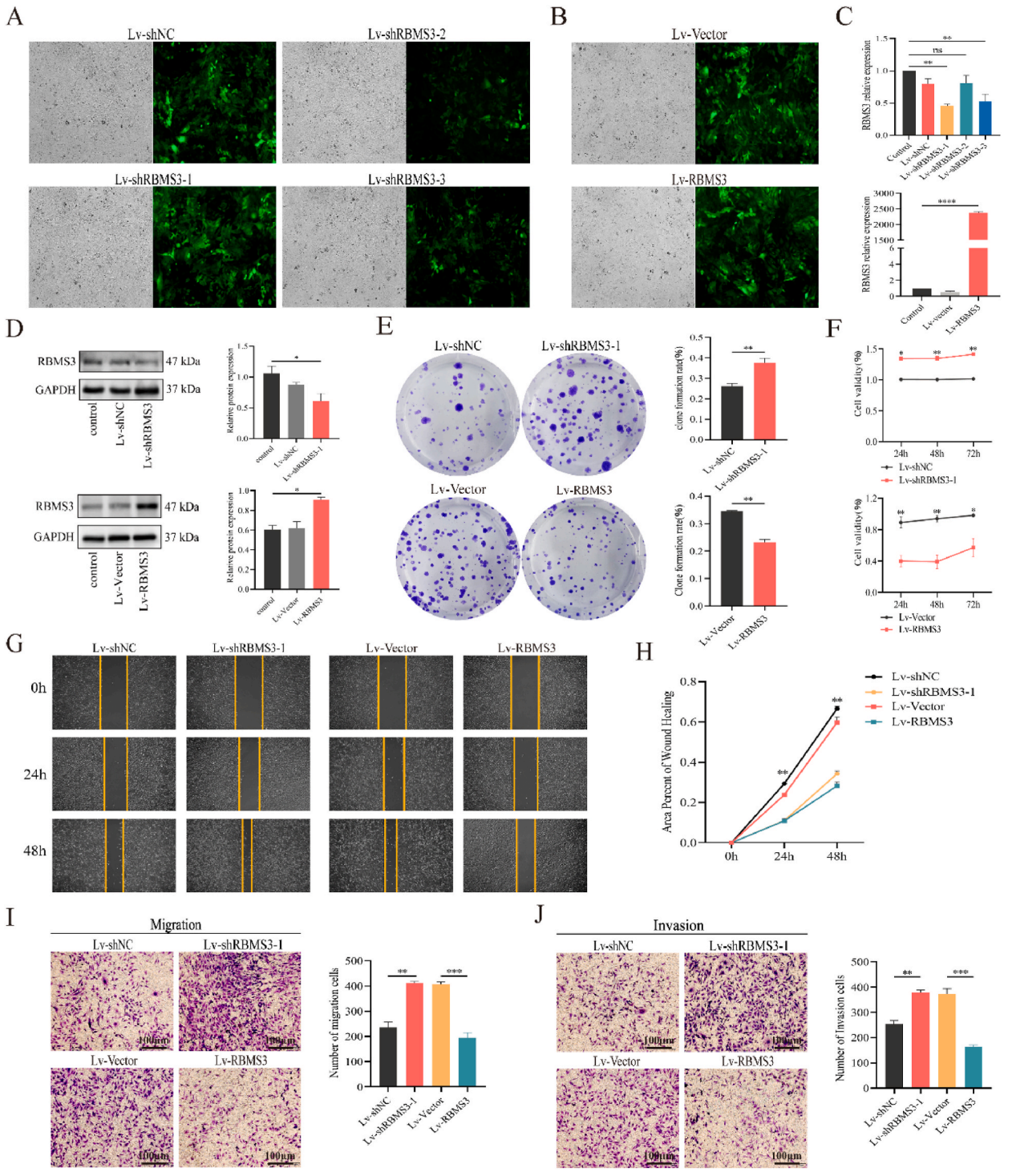

Fig. 2. The overexpression and suppression of the RBMS3 gene can control the capabilities to migrate, invade, and reproduce of OC cells. (A, B) Stable ID8 cell lines that overexpress and knockdown RBMS3 were created using the lentiviral transfection approach. The fluorescence plot illustrates representative images of stably transfected cells in both dark and bright settings (Microscopic magnification: 20 ×). (C) Comparative mRNA expression levels of RBMS3 in lentiviral-transfected ID8 cells. (D) Western Blot analysis verified that ID8 cells had overexpressed and knocked down RBMS3 genes. (E, F) Plate cloning and CCK-8 were used to determine cell growth. (G, H) Experiments on wound healing demonstrate how RBMS3 affects the capacity for cell migration (Microscopic magnification: 4 ×). (I, J) The Transwell technique for identifying the capacity for the capabilities in invading and migrating of cells (Microscopic magnification: 10 ×). The scale bar is 100 μm *$P < 0.05$, **$P < 0.01$, and ***$P < 0.001$. The uncropped versions of Fig. 2D is in Supplementary Figs. S3 and S4.

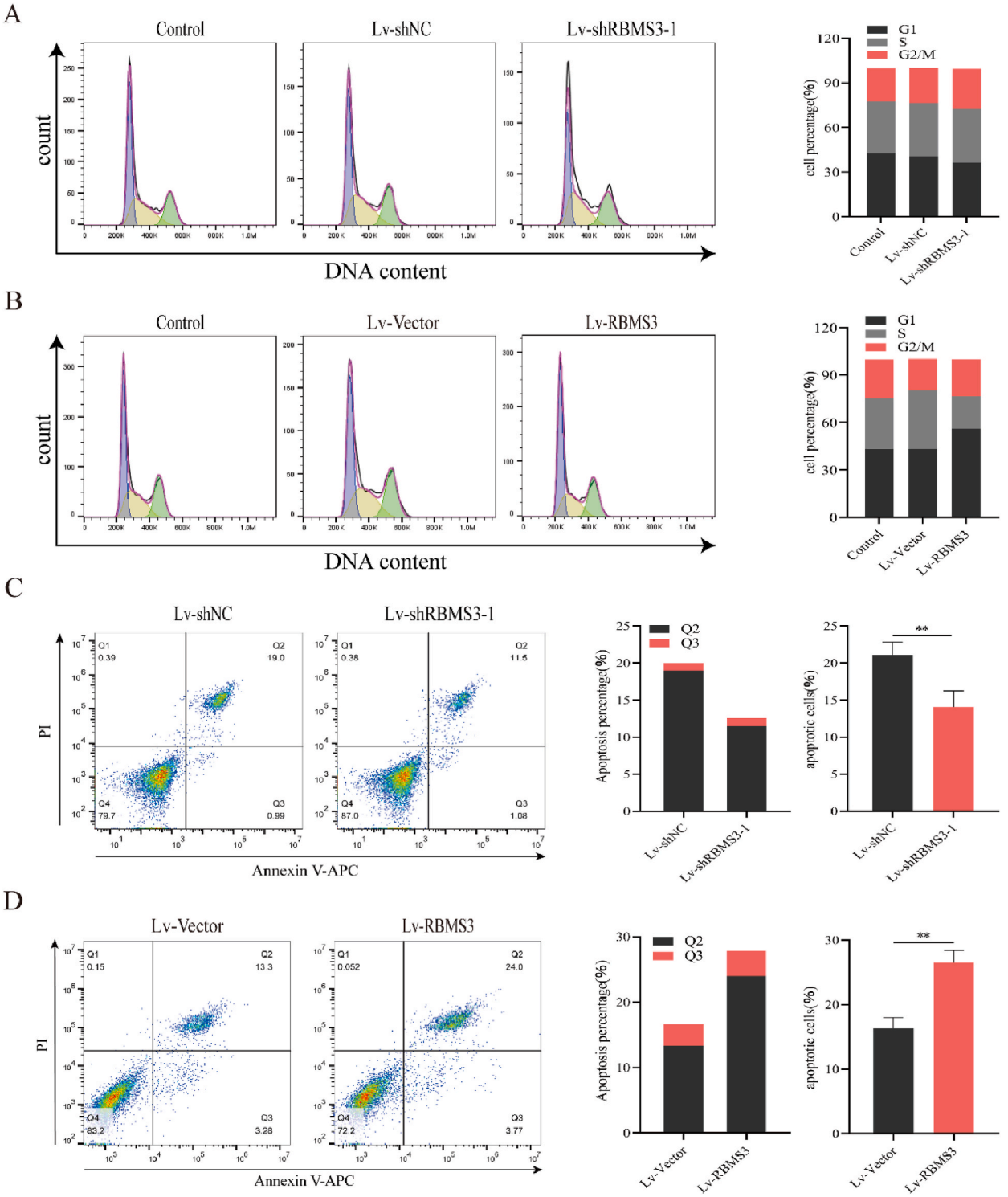

Fig. 3. The RBMS3 gene induces cell cycle arrest and apoptosis, potentially preventing the progression of OC cells. (A, B) Histograms of the flow cytometry data and flow cytometry detection of the cell cycle distribution of ID8 cells before and after RBMS3 gene overexpression and knockdown. (C, D) Using flow cytometry, the apoptotic rate of ID8 cells with RBMS3 lentivirus overexpression and knockdown was examined. $^{*}P < 0.05$, $^{**}P < 0.01$, and $^{***}P < 0.001$.

findings suggest that RBMS3 inhibits EOC cells' *in vitro* migration and invasion potential.

3.3. Impact of RBMS3 on EOC apoptosis of cells and cell cycle in vitro

To further understand RBMS3's involvement in EOC, we used flow cytometry to analyze the effect of RBMS3 on the cell cycle, and detected the role of high and low expression of RBMS3 on the apoptosis of ID8 cells using Annexin V-APC/PI dual-labelling method. Analysis revealed that RBMS3 overexpression (Lv-RBMS3) elevated the fraction of cells in the G0/G1 phase and declined the percentage of cells in the S phase in contrast to the Lv-vector group. In comparison to the Lv-shNC group, the RBMS3 knockout cell group (LvshRBMS3-1) showed a higher proportion of cells in G2/M phase, indicating cell cycle arrest in G2/M phase (Fig. 3A, 3 B). Fig. 3 illustrates that in cells overexpressing RBMS3 (Lv-RBMS3), apoptosis was considerably greater (27.77%) than in the vector group (16.58%). On the other hand, the apoptosis rate in the Lv-shNC group (19.99%) was more elevated than that in the RBMS3 knockdown group (Lv-shRBMS3-1) (12.58%) (Fig. 3C and D). When considered collectively, these findings imply that RBMS3 stimulates apoptosis, which inhibits the development of EOC cells *in vitro*.

3.4. Connection between RBMS3 expression and immune cell infiltration in OC tissues

The present investigation looked at the interaction between RBMS3 and TIME in EOC using the TISIDB and TIMER platforms. It appeared that there was a substantial correlation between RBMS3 expression and the infiltration of major immune cell types using data from the TISIDB database (Fig. 4A). Thus, the correlations between RBMS3 expression and individual immune cell types were then investigated. The results for the individual cell types were T follicular helper cells (Tfh, Rho = 0.309, P = 3.75e-08), type 1 helper T cells (Th1, Rho = 0.296, P = 1.5e-07), type 2 helper T cells (Th2, Rho = 0.3, P = 1e-07), memory B cells (Mem_B, Rho = 0.257, P = 5.38e-06), regulatory T cells (Tregs, Rho = 0.261, P = 4.02e-06), immature B cells (IMM_B, Rho = 0.223, P = 8.5e-05), central memory CD8 T cells (Tcm_CD8, Rho = 0.232, P = 4.21e-05), central memory CD4 T cells (Tcm_CD4, Rho = 0.233, P = 3.92e-05), effector memory CD8 T cells (Tem_CD8, Rho = 0.245, P = 1.56e-05), activated B cells (Act_B, Rho = 0.191, P = 0.000764), effector memory

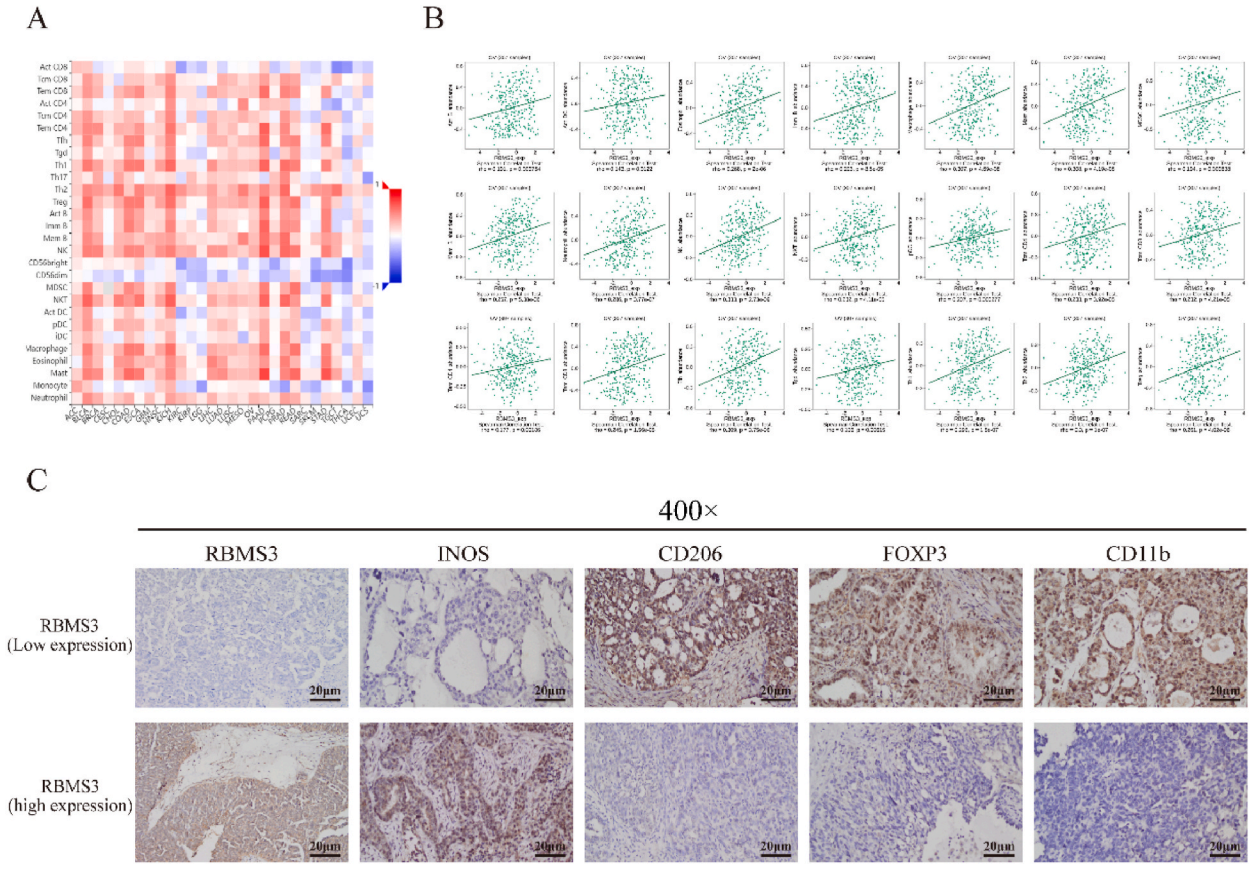

Fig. 4. Immune cell infiltration and RBMS3 expression are correlated in OC tissues. (A) TISIDB database data shows the connection between RBMS3 expression and 28 tumor-infiltrating immune cells in human cancer (red indicates positive infiltration, blue indicates negative). (B) The degree of immune cell infiltration in OC tissues is correlated with the expression of RBMS3. (C) An IHC staining diagram showing the relationship between immune cell-related markers and RBMS3 expression (magnification: 400 ×). The scale bar is 20 μm.

CD4 T cells (Tem_CD4, Rho = 0.177, P = 0.00186), activated dendritic cells (Act_DC, Rho = 0.143, P = 0.0122); NK cells (NK, Rho = 0.333, P = 2.73e-09), macrophages (macrophages, Rho = 0.307, P = 4.69e-08), mast cells (Mast, Rho = 0.308, P = 4.19e-08), neutrophils (neutrophils, Rho = 0.286, P = 3.77e-07), eosinophils (Eosinophil, Rho = 0.268, P = 2e-06) natural killer T cells (NKT, Rho = 0.232, P = 4.11e-05), myeloid-derived suppressor cells (MDSCs, Rho = 0.194, P = 0.00063), and plasmacytoid dendritic cells (pDCs, Rho = 0.207, P = 0.000277) (Fig. 4B). In order to profoundly delve into the connection between tumor immunity and RBMS3 expression, correlations were assessed between immune cell markers linked to Tregs, M1 macrophages, M2 macrophages, and MDSCs and RBMS3 expression. High expression of RBMS3 was shown to be negatively connected with Tregs, MDSCs, and M2 macrophages, and positively correlated with M1 macrophages, according to the immune cell labeling data (Fig. 4C and D).

3.5. *Cellular experiments validates the relationship between the immune microenvironment of EOC and RBMS3 expression*

In this part, cellular immunofluorescence assay was used to detect the regulatory effects of RBMS3 on Tregs, MDSCs, M1 and M2 macrophages. The cell samples were divided into two groups, Lv-vector and Lv-RBMS3 (Fig. 5A and B), and the expression levels of immune cell markers INOS, ARG1, FOXP3 and CD11b were compared between the two groups, respectively. The results showed that compared with Lv-vector, the expression of M1-type macrophage markers was higher in the RBMS3 high-expression group, while the

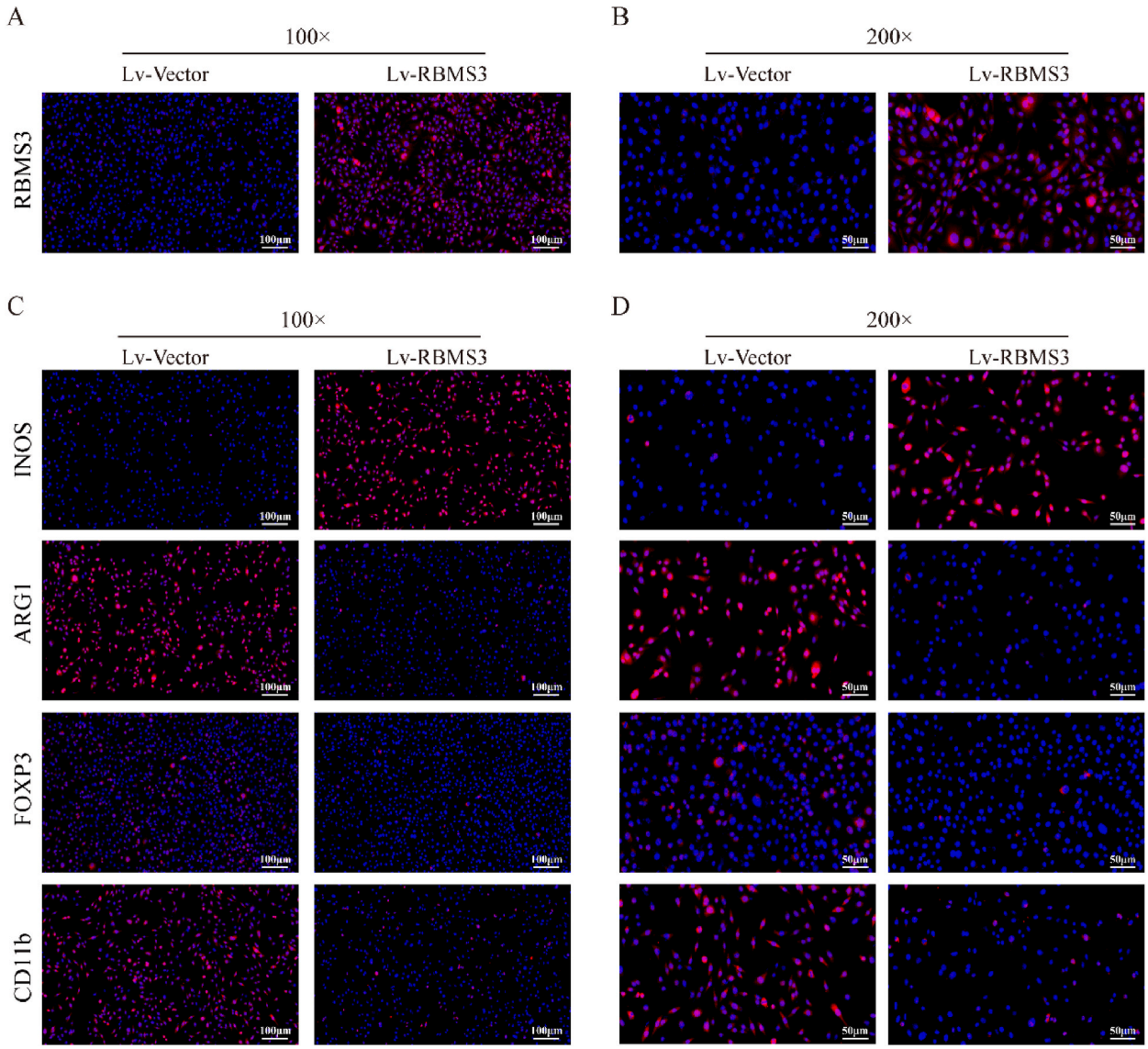

Fig. 5. The relationship between high and low RBMS3 expression in ID8 cells and immune cell markers. (A,B) RBMS3 expression in ID8 cells in both groups. (C,D) Immunofluorescence imagesof INOS, ARG1, FOXP3 and CD11b in cells of Lv-Vector and Lv-RBMS3 groups (200 × and 400 ×). The scale bars are 100 μm and 50 μm respectively.

levels of markers were lower in M2-type macrophages, Tregs and MDSCs (Fig. 5C and D).

3.6. Experiments on synthetic transplanted tumors validated RBMS3's anti-tumor activity in vivo

Using syngeneic transplanted animal models, the anti-tumor growth effects of RBMS3 were examined *in vivo*. The tumor volumes were determined and the mice were weighed when noticeable bulges were apparent beneath the skin. Tumor weights and volumes were lower in the RBMS3 overexpression group, which is in line with the *in vitro* outcomes (Fig. 6A–D). The findings of Ki-67 immunohistochemistry staining also demonstrated that overexpression of RBMS3 inhibited tumor development (Fig. 6E). By using CD31 histochemical staining to assess tumor angiogenesis, the findings showed less positive staining in the Lv-RBMS3 group compared to the vector group, suggesting that RBMS3 overexpression inhibited the tumor blood vessel formation (Fig. 6F).

3.7. Animal experiments validates the association between EOC's immunological milieu and RBMS3 expression

Evaluations were conducted on the regulatory effects of RBMS3 on Tregs, MDSCs, M1 and M2 macrophages. The tumor tissue samples were separated into two groups of low and high expression in terms of the IHC-determined expression of RBMS3 (Fig. 7A and B), and the two groups' levels of the immune cell markers INOS, ARG1, FOXP3, and CD11b were compared. In line with earlier findings, the RBMS3 overexpression group showed higher expression of M1-type macrophage markers as in contrast to the control group, whereas lower levels of markers for M2-type macrophages, Tregs, and MDSCs were observed (Fig. 7C and D).

3.8. Effects of RBMS3 on the Wnt/β-catenin signalling pathway in ovarian cancer cells

To further explore the mechanism of action of RBMS3, we evaluated the expression of β-catenin, a key protein in the Wnt/β-catenin signalling pathway. Western Blot results showed that overexpression of RBMS3 inhibited the expression level of β-catenin in ID8 cells (Fig. 8A and B). Transwell migration and invasion The results of the experiments showed that SKL2001, an agonist of β-catenin, abrogated the inhibition of cell migration and invasion by RBMS3 overexpression (Fig. 8C and D).

4. Discussion

One of the most prevalent gynecological diseases, ovarian cancer has a history of high morbidity and death rates. The current two prevalent treatments for ovarian cancer are surgery and chemotherapy. The survival rates of individuals with ovarian cancer have not

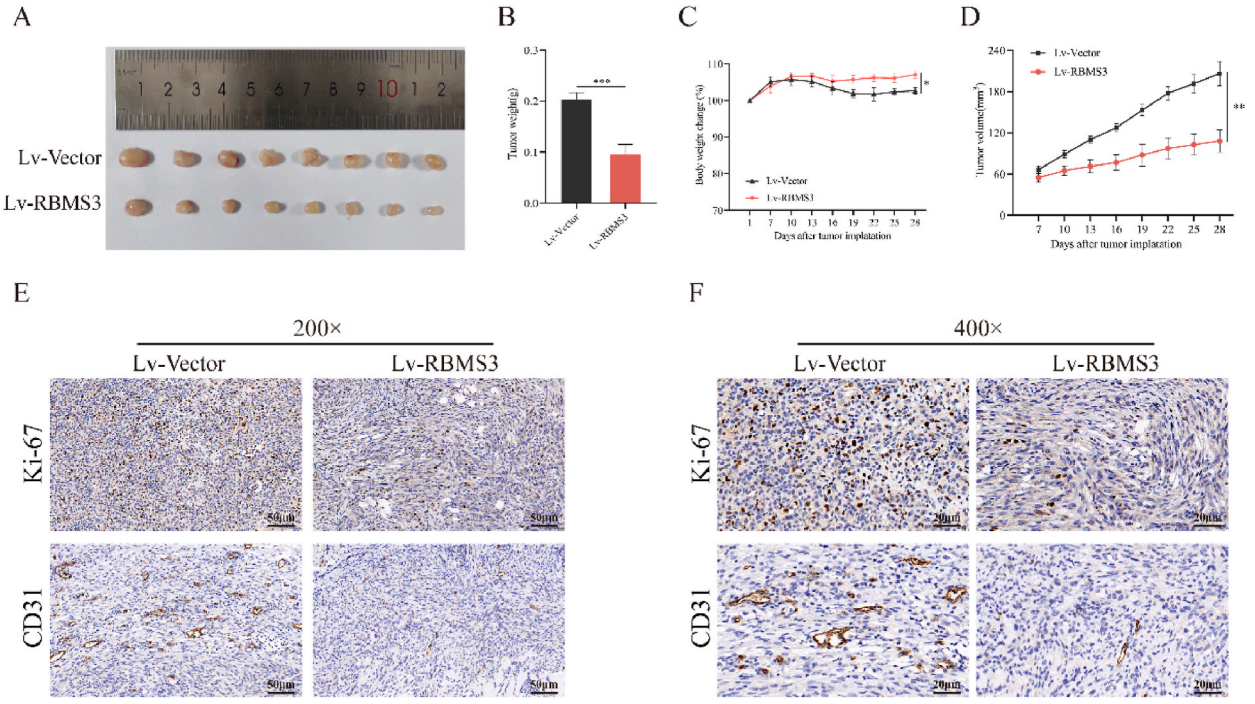

Fig. 6. Impact of overexpressing the RBMS3 gene on *in vivo* angiogenesis and tumor growth. (A) Diagram of mouse subcutaneous tumor growth. (B) Tumor weight 28 days after inoculating cells. (C) Mouse weight growth curve. (D) Measure the subcutaneous tumor volume, tumor volume = 0.5 × largest dimension × shortest dimension^2. (E, F) Immunohistochemistry (IHC) staining of Ki-67 and CD31 in transplanted tumor tissue Lv-Vector and Lv-RBMS3 groups (200 × and 400 ×). The scale bars are 50 μm and 20 μm respectively.

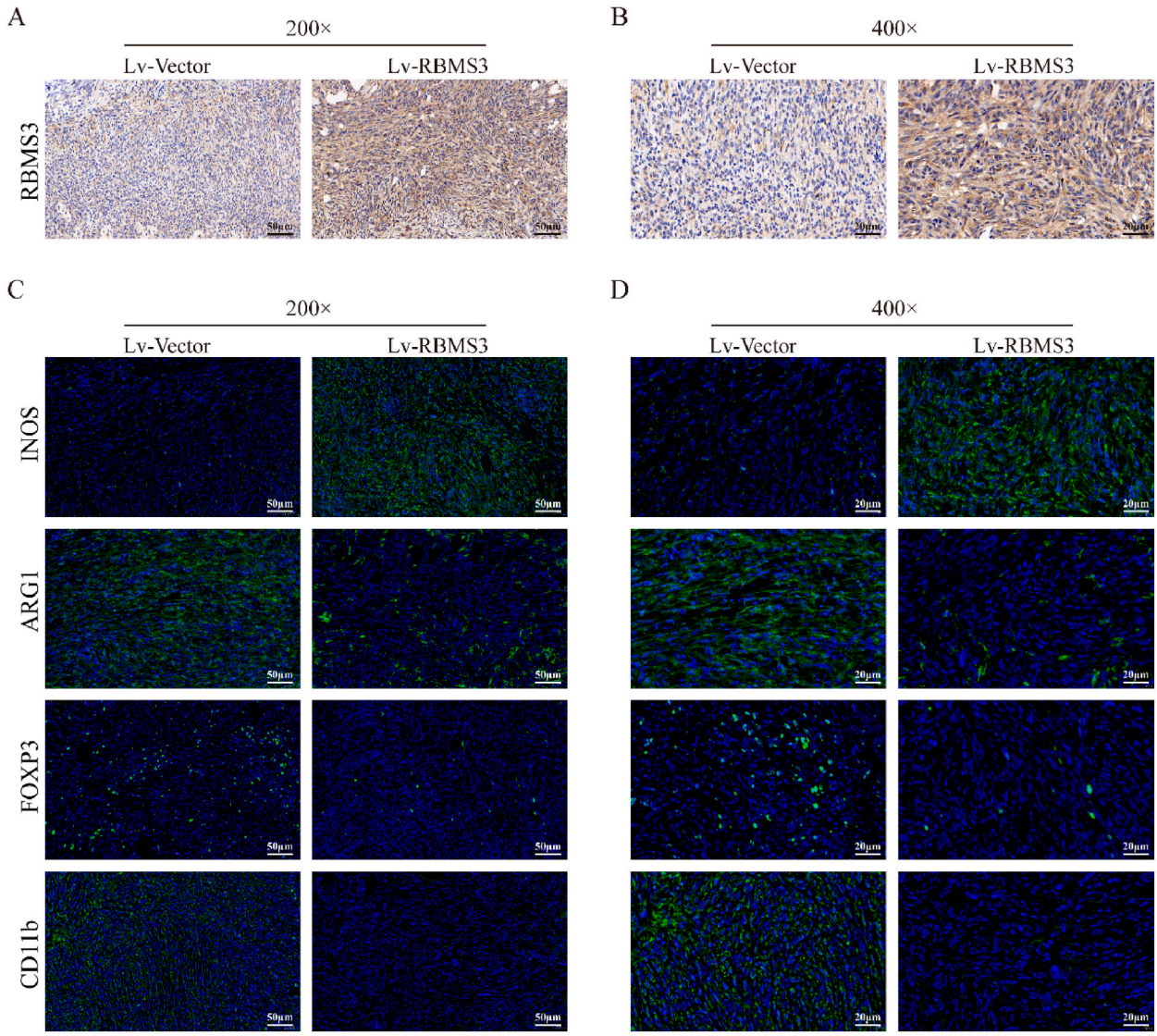

Fig. 7. The relationship between high and low expression of RBMS3 in tumor tissues and immune cell markers. (A,B) IHC staining detects the expression of RBMS3 in mouse tumor tissues. (C,D) Immunofluorescence detection images of INOS, ARG1, FOXP3 and CD11b in the Lv-Vector and Lv-RBMS3 groups of transplanted tumor tissues (200 × and 400 ×). The scale bars are 50 μm and 20 μm respectively.

increased as a result of these therapies, albeit [27]. For this reason, finding trustworthy biomarkers is essential to enhancing the prognosis of EOC, and developing novel therapies is crucial. The RNA-binding protein RBMS3 is located at 3p24–23. Many solid tumors are discovered to have deleted or altered regions on the short arm of chromosome 3, which represent hotspots of genetic change and may harbor one or more oncogenes [28]. Though there is increasing evidence that points to RBMS3 as a possible therapeutic target, it is still unclear how RBMS3 functions and what role it plays in the onset and spread of EOC, especially concerning tumor immunology. We have demonstrated the prognostic significance of RBMS3 in this study and have identified it as a tumor suppressor in EOC. Studies have been conducted regarding the function of RBMS3 in the onset and progression of EOC. The study's conclusions showed that while RBMS3 overexpression promoted cell death, it prevented EOC cell growth, invasion, migration, and other pathological activities. Simultaneously, the analysis also focused on the possible influence of RBMS3 expression on immune cell infiltration within the TME.

It is thought that RBMS3 may be a tumor suppressor since tumor tissues and cells, such as nasopharyngeal carcinoma [29,30], breast cancer [31], and lung cancer [24], express less of this protein. The current research verified that RBMS3 was dramatically downregulated in the tissues of EOC patients. Using a variety of experimental techniques, such as qPCR, Western blotting, and IHC, RBMS3 expression at both the mRNA and protein levels was assessed and analyzed in EOC tissue and normal ovarian tissue. According to the findings revealed, EOC tissue had dramatically lower levels of RBMS3 expression ($P < 0.05$). Data from the GEPIA database were also examined in order to corroborate these results. Moreover, according to the findings, EOC tissues had decreased RBMS3 expression.

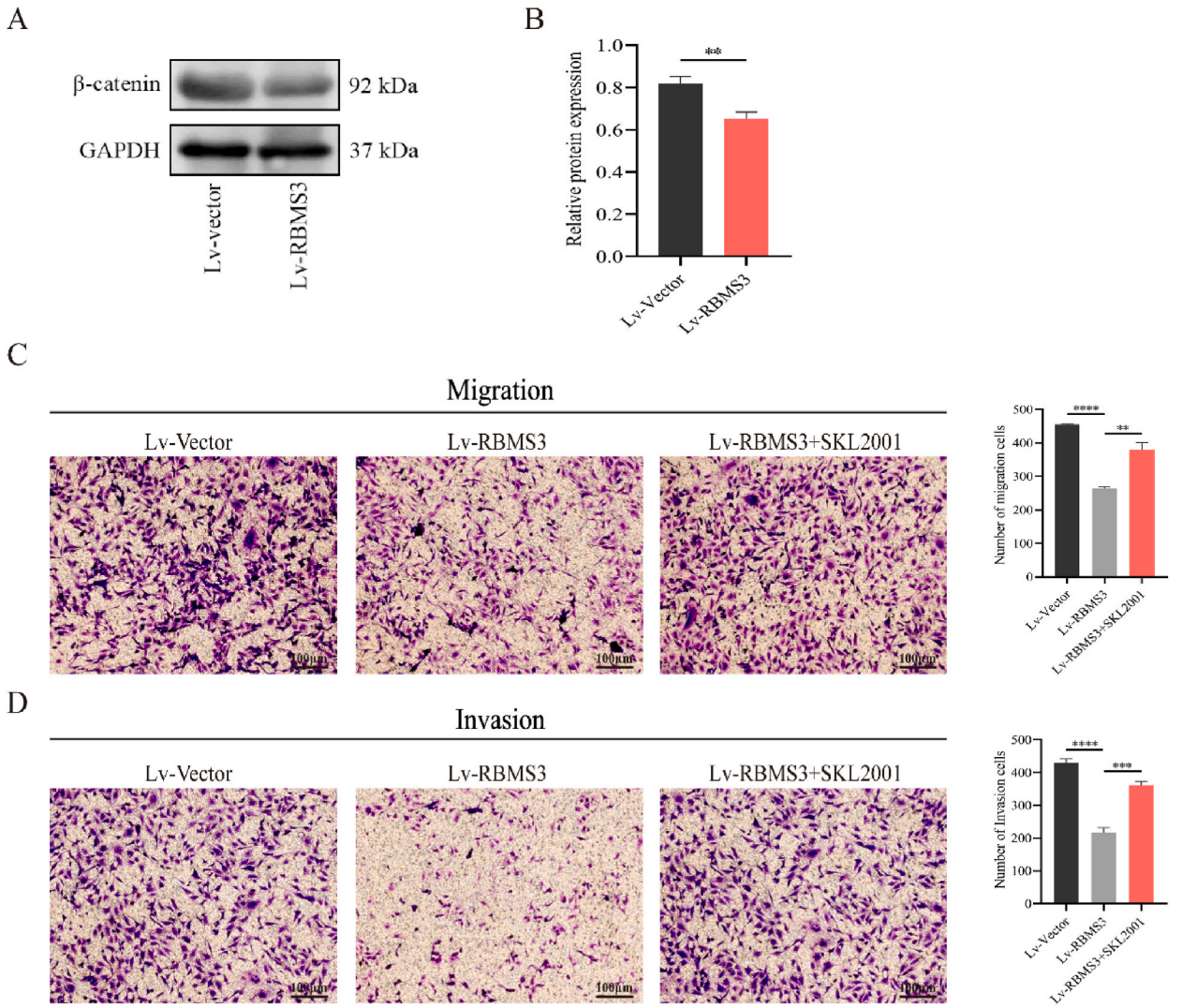

Fig. 8. Effects of RBMS3 on the Wnt/β-catenin signalling pathway in ovarian cancer cells. (A, B) Up-regulation of RBMS3 regulates the Wnt/β-catenin signalling pathway in ID8 cells. (C) After overexpression of RBMS3 and activation of the Wnt/β-catenin signalling pathway, the migratory activity of ID8 cells was detected by transwell. (D) After overexpression of RBMS3 and activation of the Wnt/β-catenin signalling pathway, the invasive activity of ID8 cells was detected by transwell. The scale bars is 100 μm $^{**}P < 0.01$, $^{***}P < 0.001$ and $^{****}P < 0.0001$. The uncropped versions of Fig. 8A is in Supplementary Fig. S5.

These outcomes also align with earlier research on EOC conducted by Wang et al. [26]. Notably, low expression of RBMS3 was linked to poorer OS (HR = 0.410, P = 0.0431) and PFS (HR = 0.3778, P = 0.0329), according to the Kaplan-Meier plotter database and survival curves. This suggests that RBMS3 may be an effective prognostic biomarker for EOC. Moreover, research has demonstrated that RBMS3 is crucial for the development of tumors and angiogenesis. Targeting Caspase-9, PARP, and MMP2, RBMS3 was reported to dramatically enhance apoptosis and limit microvessel development in nasopharyngeal cancer cells [30]. It has been demonstrated that RBMS3 is essential for the preservation of the mesenchymal phenotype and the tumor cells' capacity to penetrate and migrate in breast cancer [32]. Activation of AMPK in lung cancer leads to the overexpression of RBMS3 and prevents the tumor cells from migrating, invading, and proliferating [24]. The findings of the present study comply with the data from these investigations. Research has indicated that RBMS3 overexpression adversely controls cell invasion, migration, and proliferation while also encouraging apoptosis; in contrast, RBMS3 knockdown has the reverse impact and also affects the cell cycle. Furthermore, the current investigation verified that angiogenesis and EOC cell proliferation are linked to elevated RBMS3 expression. Using a subcutaneous tumor xenograft mouse model, these findings were verified. These findings suggest that RBMS3 has anti-tumor characteristics in EOC and that regulating its expression might be a useful therapeutic target to treat the condition.

The Wnt/β-catenin signalling pathway is considered an oncogenic pathway in the development of many cancers [22]. It has been shown that RBMS3 inhibits tumourigenesis and breast cancer cell proliferation and migration through inactivation of the Wnt/β-catenin signalling pathway [33]. Wang et al. [23] have also suggested that RBMS3 inhibits the Wnt/β-catenin signalling

pathway, enhances the proliferation of nucleus pulposus cells, inhibits apoptosis and inflammation, and therefore delays intervertebral disc degeneration. It has also been shown that RBMS3 deficiency promotes exocytosis and induces EOC chemoresistance by a mechanism related to activation of the Wnt/β-catenin pathway [25]. Our findings are consistent with the above, and we hypothesise that the effects of RBMS3 overexpression on ID8 cell migration and invasion are mediated through the Wnt/β-catenin pathway. To verify this possibility, we used the activator SKL2001 to conduct subsequent experiments. The results showed that up-regulation of RBMS3 inhibited the activation of the Wnt/β -catenin signalling pathway, which promoted the migration and invasion of ovarian cancer cells. This suggests that Wnt/β-catenin signalling plays an important role in the action of RBMS3 on ovarian cancer cell growth. There are also many studies showing that the Wnt/β-catenin pathway has been identified as one of the important oncogenic signalling pathways associated with immune evasion [34,35], and its role in regulating immune cell infiltration in the tumor microenvironment has received increasing attention, so in-depth studies on the role of the Wnt/β-catenin pathway in cancer-related immune regulation may bring this therapeutic field bring new contents.

The TME is a dynamic, complicated environment. The TME serves as a conduit for the illness throughout the body, and it is becoming more well-recognized for its part in the progression and spread of EOC as well as the use of anti-tumor therapies [36,37]. Although the TME's composition varies according to the kind of tumor, tumor and stromal cells, extracellular matrix, and immune cells that have infiltrated the tissue are its most important constituents [38]. Tumor-infiltrating immune cells (TIICs) have been linked to tumor formation and initiation, immune escape, and the promotion and maintenance of an immunosuppressive microenvironment, given several recent studies [39]. It has been demonstrated that Tregs in ovarian cancer contribute to resistance and cancer progression at various disease stages. Knutson et al. [40] [][][]revealed that in ovarian cancer, $CD4^{+}CD25^{+}FOXP3^{+}$ regulatory T cells frequently infiltrate the microenvironment, leading to anti-tumor immune suppression. Increased levels of tumor-infiltrating MDSCs were reported to be dramatically linked to a shorter survival time in patients with highly serous ovarian cancer, according to Cui et al. [41]. These cells are a significant source of immunosuppression in EOC. Baert et al. [42] found that MDSCs reduced the activities of effector T cells and created adverse immunological characteristics that grew with the tumor's growth in a mouse model of ovarian cancer. MicroRNAs (miRNAs) can cause an imbalance between Th17 and Treg cells in exosomes produced by TAMs. This imbalance can contribute to the establishment of an immunosuppressive milieu, which thus encourages EOC advancement and metastasis, as noted by Zhou et al. [43]. The TAMs are crucial elements of the TME. Based on how they react to various stimuli, macrophages may be broadly classified into two phenotypes, pro-tumor M2 type as well as anti-tumor M1 type [44]. Different functions are played by M1 and M2 macrophages in malignancies. M2 macrophages help tumor cells avoid immune assault and promote tumor growth and spread. They are linked to the suppressive immunological environment in the tumor microenvironment (TME). Conversely, M1 macrophages can stimulate immunological responses that are anti-tumor [45]. We examined the connection between RBMS3 and immune infiltration in OC further using internet databases. This demonstrated that the invasion of several immune cell types, such as Tfh, Tregs, $CD8^{+}$ T cells, $CD4^{+}$ T cells, B cells, NK cells, macrophages, neutrophils, eosinophils, and myeloid-derived suppressor cells, was positively correlated with ovarian RBMS3 expression. This outcome reveals that RBMS3 may have a positive impact role in controlling the invasion of immune cells in EOC. Additionally, Zhou et al. [46] demonstrated that RBMS3 deletion improved T cell-mediated tumor death *in vivo*, indicating a critical function for RBMS3 in the control of immune surveillance. Additionally, it was discovered that RBMS3 had a substantial negative connection with M2-type macrophages (CD206/ARG1), Tregs (FOXP3), and MDSCs (CD11b), and a positive association with M1-type macrophages (INOS) in a later immune cell marker correlation study. When combined, the TME's dynamic characteristics, tumor-infiltrating cells, and immunological biomarkers have a major impact on how well a patient responds to immunotherapy [47]. The results of these investigations also demonstrated the critical function of RBMS3 in controlling TIME, offering further insight into the protein's potential as a prognostic indicator and therapeutic target. Even yet, to completely comprehend the complexity and therapeutic significance of RBMS3 in the immunological environment, more investigation is required.

While this study contributes to the investigation of the connection between RBMS3 and EOC, it has significant drawbacks. Initially, the EOC cohort study's sample size was quite modest; bigger and longer follow-up studies are required to provide more precise findings. Secondly, the regulatory mechanisms need to be explored more deeply; thus, more research on the mechanism of action of the Wnt/β-catenin pathway in relation to ovarian cancer-associated immunomodulation are needed in the future, which is expected to lay the foundation for immunotherapy targeting ovarian cancer.

5. Conclusion

In summary, the study's findings verified that RBMS3 expression was downregulated in EOC and that it had a substantial connection with the prognosis of individuals with EOC. This implies that deeper investigations on RBMS3 as a biomarker for EOC prognosis would be worthwhile. Furthermore, it was discovered that RBMS3 overexpression mediated the TIME and was connected to immune cell infiltration. The biological activities of EOC cells and immune infiltration of the EOC TME are both impacted by dysregulation of RBMS3, which also has a major effect on the advancement of EOC. Despite many limitations in the study, the results are noteworthy and establish a foundation for further investigation into the molecular processes behind RBMS3 activity and its potential as a therapeutic target. These investigations would build the groundwork and demonstrate RBMS3's potential as a pivotal figure in cancer biology and treatment.

Funding

This study was supported by the Natural Science Fund for Colleges and Universities of Anhui Province [No. KJ2021A0727] and the Graduate Student Research and Innovation Program of Bengbu Medical College [No. Byycx22047].

Data availability statement

The bioinformatics datasets generated and/or analyzed during the current study are available in Gene Expression Profiling Interactive Analysis (GEPIA) (http://gepia.cancer-pku.cn/) and the TISIDB (http://cis.hku.hk/TISIDB/index.php). Datasets 242,137_at on OS and PFS are available in Kaplan-Meier plotter (https://kmplot.com/analysis/). The datasets used and analyzed during the current study are available from the corresponding author on reasonable request.

CRediT authorship contribution statement

Tian Yin: Writing – review & editing, Writing – original draft. **Ying Zhang:** Writing – review & editing, Conceptualization. **Yue Zhao:** Data curation. **Xinyi Zhang:** Formal analysis. **Shuqi Han:** Methodology, Investigation. **Yixiao Wang:** Software, Resources. **Bo Yang:** Project administration, Funding acquisition.

Declaration of competing interest

The authors declare that they have no known competing financial interests or personal relationships that could have appeared to influence the work reported in this paper.

Appendix A. Supplementary data

Supplementary data to this article can be found online at https://doi.org/10.1016/j.heliyon.2024.e30603.

References

[1] C.J. Cabasag, P.J. Fagan, J. Ferlay, J. Vignat, M. Laversanne, L. Liu, M.A. van der Aa, F. Bray, I. Soerjomataram, Ovarian cancer today and tomorrow: a global assessment by world region and Human Development Index using GLOBOCAN 2020, Int. J. Cancer 151 (9) (2022) 1535–1541, https://doi.org/10.1002/ijc.34002.
[2] V. Garg, A.-M. Oza, Treatment of ovarian cancer beyond PARP inhibition: current and future options, Drugs 83 (15) (2023) 1365–1385, https://doi.org/10.1007/s40265-023-01934-0.
[3] L. Kuroki, S.R. Guntupalli, Treatment of epithelial ovarian cancer, BMJ 371 (2020) m3773, https://doi.org/10.1136/bmj.m3773.
[4] J. Xiong, J.Y. Chen, X. Sun, R. Zhao, K.F. Gao, Prognostic role of long non-coding RNA USP30-AS1 in ovarian cancer: insights into immune cell infiltration in the tumor microenvironment, Aging-Us 15 (23) (2023) 13776–13798, https://doi.org/10.18632/aging.205262.
[5] K. Odunsi, Immunotherapy in ovarian cancer, Ann. Oncol. 28 (2017) viii1–viii7, https://doi.org/10.1093/annonc/mdx444.
[6] A. Rajtak, M. Ostrowska-Lesko, K. Zak, R. Tarkowski, J. Kotarski, K. Okla, Integration of local and systemic immunity in ovarian cancer: implications for immunotherapy, Front. Immunol. 13 (2022) 1018256, https://doi.org/10.3389/fimmu.2022.1018256.
[7] Z.R.C. Marks, N.K. Campbell, N.E. Mangan, C.J. Vandenberg, L.J. Gearing, A.Y. Matthews, J.A. Gould, M.D. Tate, G. Wray-McCann, L. Ying, S. Rosli, N. Brockwell, B.S. Parker, S.S. Lim, M. Bilandzic, E.L. Christie, A.N. Stephens, E. de Geus, M.J. Wakefield, G.Y. Ho, O. McNally, A.O.C. Study, I.A. McNeish, D.D. L. Bowtell, N.A. de Weerd, C.L. Scott, N.M. Bourke, P.J. Hertzog, Interferon-epsilon is a tumour suppressor and restricts ovarian cancer, Nature 620 (7976) (2023) 1063–1070, https://doi.org/10.1038/s41586-023-06421-w.
[8] H.H. Chen, K.Q. Yang, L.X. Pang, J. Fei, Y.L. Zhu, J.W. Zhou, ANKRD22 is a potential novel target for reversing the immunosuppressive effects of PMN-MDSCs in ovarian cancer, J Immunother Cancer 11 (2023), https://doi.org/10.1136/jitc-2022-005527. ARTN e005527.
[9] N.M. Anderson, M.C. Simon, The tumor microenvironment, Curr. Biol. 30 (16) (2020) R921–R925, https://doi.org/10.1016/j.cub.2020.06.081.
[10] F. De Felice, C. Marchetti, I. Palaia, D. Musio, L. Muzii, V. Tombolini, P.B. Panici, Immunotherapy of ovarian cancer: the role of checkpoint inhibitors, J Immunol Res 2015 (2015) 191832, https://doi.org/10.1155/2015/191832.
[11] K.E. de Visser, J.A. Joyce, The evolving tumor microenvironment: from cancer initiation to metastatic outgrowth, Cancer Cell 41 (3) (2023) 374–403, https://doi.org/10.1016/j.ccell.2023.02.016.
[12] D. Penkov, R. Ni, C. Else, S. Pinol-Roma, F. Ramirez, S. Tanaka, Cloning of a human gene closely related to the genes coding for the c-myc single-strand binding proteins, Gene 243 (1–2) (2000) 27–36, https://doi.org/10.1016/s0378-1119(99)00515-6.
[13] T. Niki, S. Izumi, Y. Saegusa, T. Taira, T. Takai, S.M. Iguchi-Ariga, H. Ariga, MSSP promotes ras/myc cooperative cell transforming activity by binding to c-Myc, Gene Cell. 5 (2) (2000) 127–141, https://doi.org/10.1046/j.1365-2443.2000.00311.x.
[14] D. Fritz, B. Stefanovic, RNA-binding protein RBMS3 is expressed in activated hepatic stellate cells and liver fibrosis and increases expression of transcription factor Prx1, J. Mol. Biol. 371 (3) (2007) 585–595, https://doi.org/10.1016/j.jmb.2007.06.006.
[15] C.K. Lu, Y.C. Lai, H.R. Chen, M.K. Chiang, Rbms3, an RNA-binding protein, mediates the expression of Ptf1a by binding to its 3'UTR during mouse pancreas development, DNA Cell Biol. 31 (7) (2012) 1245–1251, https://doi.org/10.1089/dna.2012.1619.
[16] P. Nicoletti, V.M. Cartsos, P.K. Palaska, Y. Shen, A. Floratos, A.I. Zavras, Genomewide pharmacogenetics of bisphosphonate-induced osteonecrosis of the jaw: the role of RBMS3, Oncol. 17 (2) (2012) 279–287, https://doi.org/10.1634/theoncologist.2011-0202.
[17] Y. Li, L. Chen, C.J. Nie, T.T. Zeng, H. Liu, X. Mao, Y. Qin, Y.H. Zhu, L. Fu, X.Y. Guan, Downregulation of RBMS3 is associated with poor prognosis in esophageal squamous cell carcinoma, Cancer Res. 71 (19) (2011) 6106–6115, https://doi.org/10.1158/0008-5472.CAN-10-4291.
[18] Y.N. Liang, Y. Liu, Q. Meng, X. Li, F. Wang, G. Yao, L. Wang, S. Fu, D. Tong, RBMS3 is a tumor suppressor gene that acts as a favorable prognostic marker in lung squamous cell carcinoma, Med. Oncol. 32 (2) (2015) 459, https://doi.org/10.1007/s12032-014-0459-9.
[19] T. Zhang, Y. Wu, Z. Fang, Q. Yan, S. Zhang, R. Sun, J. Khaliq, Y. Li, Low expression of RBMS3 and SFRP1 are associated with poor prognosis in patients with gastric cancer, Am. J. Cancer Res. 6 (11) (2016) 2679–2689. PMID:27904780.
[20] Y. Wu, D. Meng, Y. You, R. Sun, Q. Yan, J. Bao, Y. Sun, D. Yun, Y. Li, D. Sun, Increased expression of RBMS3 predicts a favorable prognosis in human gallbladder carcinoma, Oncol. Rep. 44 (1) (2020) 55–68, https://doi.org/10.3892/or.2020.7594.
[21] C. Wang, Y. Wu, Y. Liu, F. Pan, H. Zeng, X. Li, L. Yu, Tumor suppressor effect of RBMS3 in breast cancer, Technol. Cancer Res. Treat. 20 (2021) 1–9, https://doi.org/10.1177/15330338211004921.
[22] T. Gornicki, J. Lambrinow, M. Mrozowska, M. Podhorska-Okolow, P. Dziegiel, J. Grzegrzolka, Role of RBMS3 novel potential regulator of the EMT phenomenon in physiological and pathological processes, Int. J. Mol. Sci. 23 (2022) 10875, https://doi.org/10.3390/ijms231810875.

[23] J.J. Wang, X.Y. Liu, W. Du, J.Q. Liu, B. Sun, Y.P. Zheng, RBMS3 delays disc degeneration by inhibiting Wnt/beta-catenin signaling pathway, Eur. Rev. Med. Pharmacol. Sci. 24 (2) (2020) 499–507, https://doi.org/10.26355/eurrev_202001_20023.
[24] S.L. Lv, X. Zhou, Y.J. Li, L.Y. Luo, D.Q. Huang, RBMS3, a downstream target of AMPK, exerts inhibitory effects on invasion and metastasis of lung cancer, J. Cancer 14 (15) (2023) 2784–2797, https://doi.org/10.7150/jca.86572.
[25] G. Wu, L. Cao, J. Zhu, Z. Tan, M. Tang, Z. Li, Y. Hu, R. Yu, S. Zhang, L. Song, J. Li, Loss of RBMS3 confers platinum resistance in epithelial ovarian cancer via activation of miR-126-5p/beta-catenin/CBP signaling, Clin. Cancer Res. 25 (3) (2019) 1022–1035, https://doi.org/10.1158/1078-0432.CCR-18-2554.
[26] M. Wang, X. Fu, W. Wang, Y. Zhang, Z. Jiang, Y. Gu, M. Chu, Y. Shao, S. Li, Comprehensive bioinformatics analysis confirms RBMS3 as the central candidate biological target for ovarian cancer, Med. Eng. Phys. 110 (2022) 103883, https://doi.org/10.1016/j.medengphy.2022.103883.
[27] D.K. Armstrong, R.D. Alvarez, J.N. Bakkum-Gamez, L. Barroilhet, K. Behbakht, A. Berchuck, J.S. Berek, L.M. Chen, M. Cristea, M. DeRosa, A.C. ElNaggar, D. M. Gershenson, H.J. Gray, A. Hakam, A. Jain, C. Johnston, C.A. Leath III, J. Liu, H. Mahdi, D. Matei, M. McHale, K. McLean, D.M. O'Malley, R.T. Penson, S. Percac-Lima, E. Ratner, S.W. Remmenga, P. Sabbatini, T.L. Werner, E. Zsiros, J.L. Burns, A.M. Engh, NCCN guidelines insights: ovarian cancer, version 1.2019, J. Natl. Compr. Cancer Netw. 17 (8) (2019) 896–909, https://doi.org/10.6004/jnccn.2019.0039.
[28] H. Hong, H. Zhu, S. Zhao, K. Wang, N. Zhang, Y. Tian, Y. Li, Y. Wang, X. Lv, T. Wei, Y. Liu, S. Fan, Y. Liu, Y. Li, A. Cai, S. Jin, Q. Qin, H. Li, The novel circCLK3/miR-320a/FoxM1 axis promotes cervical cancer progression, Cell Death Dis. 10 (12) (2019) 950, https://doi.org/10.1038/s41419-019-2183-z.
[29] J. Chen, L. Fu, L.Y. Zhang, D.L. Kwong, L. Yan, X.Y. Guan, Tumor suppressor genes on frequently deleted chromosome 3p in nasopharyngeal carcinoma, Chin. J. Cancer 31 (5) (2012) 215–222, https://doi.org/10.5732/cjc.011.10364.
[30] J. Chen, D.L. Kwong, C.L. Zhu, L.L. Chen, S.S. Dong, L.Y. Zhang, J. Tian, C.B. Qi, T.T. Cao, A.M. Wong, K.L. Kong, Y. Li, M. Liu, L. Fu, X.Y. Guan, RBMS3 at 3p24 inhibits nasopharyngeal carcinoma development via inhibiting cell proliferation, angiogenesis, and inducing apoptosis, PLoS One 7 (9) (2012) e44636, https://doi.org/10.1371/journal.pone.0044636.
[31] T. Gornicki, J. Lambrinow, M. Mrozowska, H. Romanowicz, B. Smolarz, A. Piotrowska, A. Gomulkiewicz, M. Podhorska-Okolow, P. Dziegiel, J. Grzegrzolka, Expression of RBMS3 in breast cancer progression, Int. J. Mol. Sci. 24 (2023) 2866, https://doi.org/10.3390/ijms24032866.
[32] C.J. Block, A.V. Mitchell, L. Wu, J. Glassbrook, D. Craig, W. Chen, G. Dyson, D. DeGracia, L. Polin, M. Ratnam, H. Gibson, G. Wu, RNA binding protein RBMS3 is a common EMT effector that modulates triple-negative breast cancer progression via stabilizing PRRX1 mRNA, Oncogene 40 (46) (2021) 6430–6442, https://doi.org/10.1038/s41388-021-02030-x.
[33] Y. Yang, L. Quan, Y. Ling, RBMS3 inhibits the proliferation and metastasis of breast cancer cells, Oncol. Res. 26 (1) (2018) 9–15, https://doi.org/10.3727/096504017X14871200709504.
[34] L. Song, D. Liu, J. He, X. Wang, Z. Dai, Y. Zhao, H. Kang, B. Wang, SOX1 inhibits breast cancer cell growth and invasion through suppressing the Wnt/beta-catenin signaling pathway, APMIS 124 (7) (2016) 547–555, https://doi.org/10.1111/apm.12543.
[35] S.G. Pai, B.A. Carneiro, J.M. Mota, R. Costa, C.A. Leite, R. Barroso-Sousa, J.B. Kaplan, Y.K. Chae, F.J. Giles, Wnt/beta-catenin pathway: modulating anticancer immune response, J. Hematol. Oncol. 10 (2017) 101, https://doi.org/10.1186/s13045-017-0471-6.
[36] D.F. Quail, J.A. Joyce, Microenvironmental regulation of tumor progression and metastasis, Nat Med 19 (11) (2013) 1423–1437, https://doi.org/10.1038/nm.3394.
[37] D. Hanahan, R.A. Weinberg, Hallmarks of cancer: the next generation, Cell 144 (5) (2011) 646–674, https://doi.org/10.1016/j.cell.2011.02.013.
[38] B.A. Bhat, I. Saifi, N.A. Khamjan, S.S. Hamdani, A. Algaissi, S. Rashid, M.M. Alshehri, S.A. Ganie, M. Lohani, S.I. Abdelwahab, S.A. Dar, Exploring the tumor immune microenvironment in ovarian cancer: a way-out to the therapeutic roadmap, Expert Opin. Ther. Targets 27 (9) (2023) 841–860, https://doi.org/10.1080/14728222.2023.2259096.
[39] J. Lou, L. Wei, H. Wang, SCNN1A overexpression correlates with poor prognosis and immune infiltrates in ovarian cancer, Int. J. Gen. Med. 15 (2022) 1743–1763, https://doi.org/10.2147/IJGM.S351976.
[40] K.L. Knutson, M.J. Maurer, C.C. Preston, K.B. Moysich, K. Goergen, K.M. Hawthorne, J.M. Cunningham, K. Odunsi, L.C. Hartmann, K.R. Kalli, A.L. Oberg, E. L. Goode, Regulatory T cells, inherited variation, and clinical outcome in epithelial ovarian cancer, Cancer Immunol. Immunother. 64 (12) (2015) 1495–1504, https://doi.org/10.1007/s00262-015-1753-x.
[41] T.X. Cui, I. Kryczek, L. Zhao, E. Zhao, R. Kuick, M.H. Roh, L. Vatan, W. Szeliga, Y. Mao, D.G. Thomas, J. Kotarski, R. Tarkowski, M. Wicha, K. Cho, T. Giordano, R. Liu, W. Zou, Myeloid-derived suppressor cells enhance stemness of cancer cells by inducing microRNA101 and suppressing the corepressor CtBP2, Immunity 39 (3) (2013) 611–621, https://doi.org/10.1016/j.immuni.2013.08.025.
[42] T. Baert, A. Vankerckhoven, M. Riva, A. Van Hoylandt, G. Thirion, G. Holger, T. Mathivet, I. Vergote, A. Coosemans, Myeloid derived suppressor cells: key drivers of immunosuppression in ovarian cancer, Front. Immunol. 10 (2019) 1273, https://doi.org/10.3389/fimmu.2019.01273.
[43] J. Zhou, X. Li, X. Wu, T. Zhang, Q. Zhu, X. Wang, H. Wang, K. Wang, Y. Lin, X. Wang, Exosomes released from tumor-associated macrophages transfer miRNAs that induce a Treg/Th17 cell imbalance in epithelial ovarian cancer, Cancer Immunol. Res. 6 (12) (2018) 1578–1592, https://doi.org/10.1158/2326-6066.CIR-17-0479.
[44] R. Noy, J.W. Pollard, Tumor-associated macrophages: from mechanisms to therapy, Immunity 41 (1) (2014) 49–61, https://doi.org/10.1016/j.immuni.2014.06.010.
[45] A.A. El-Arabey, S.S. Alkhalil, S.T. Al-Shouli, M.E. Awadalla, H.W. Alhamdi, T.N. Almanaa, S. Mohamed, M. Abdalla, Revisiting macrophages in ovarian cancer microenvironment: development, function and interaction, Med. Oncol. 40 (5) (2023) 142, https://doi.org/10.1007/s12032-023-01987-x.
[46] Y. Zhou, Z. Liang, Y. Xia, S. Li, J. Liang, Z. Hu, C. Tang, Q. Zhao, Q. Gong, Y. Ouyang, Disruption of RBMS3 suppresses PD-L1 and enhances antitumor immune activities and therapeutic effects of auranofin against triple-negative breast cancer, Chem. Biol. Interact. 369 (2023) 110260, https://doi.org/10.1016/j.cbi.2022.110260.
[47] C. Kaderbhai, Z. Tharin, F. Ghiringhelli, The role of molecular profiling to predict the response to immune checkpoint inhibitors in lung cancer, Cancers 11 (2019) 201, https://doi.org/10.3390/cancers11020201.